Overview of the Recent Results of the RT-1 Magnetospheric Experiment with Levitated Superconducting Magnet

H. Saitoh, Z. Yoshida, J. Morikawa, Y. Yano, T. Mizushima, and M. Kobayashi
Graduate School of Frontier Sciences, The University of Tokyo, Kashiwanoha, Kashiwa, Chiba, JAPAN

ICC2010 , Feb 16-19, Princeton, USA

Abstract and Conclusion

- Ring Trap 1 (RT-1) is a magnetospheric experiment generated by a superconducting coil magnet.
- Research goal of RT-1 is formation of high-β plasma capable of burning advanced fusion fuels.
- Coil levitation and compensation of geomagnetic error fields improved confinement properties: $N_e \sim 8\times10^{17} m^{-3}$ local β >40% (~3.5mWb) $\tau_e \sim 100ms$ Hot electrons 1~10keV 1-10 × $10^{16} m^{-3}$
- Long confinement and fluctuation-induced inward particle diffusion was observed using NNP.
- Ion heating and formation of flowing high-β plasma are future tasks.

I. Introduction

Magnetospheric plasma confinement

- Stable confinement configuration for high-β plasma is essential for advanced fusion using $D\text{-}^3He$ or D-D.
- Spacecraft observations shows existence of flowing high-β plasma in Jovian magnetosphere.
- Ultra high-β state (possibly >1) due to the dynamic pressure of fast flow is theoretically predicted.
- Taking a hint from the astrophysical phenomenon, dipole fusion experiments are being conducted.

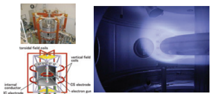

Proto-RT and Mini-RT

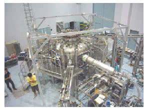

The Ring Trap 1 (RT-1) device

Yoshida *et al.*, Plasma Fusion Res. **1**, 008 (2006), Garnier *et al.*, Phys. Plasmas **13**, 056111 (2006).

Flowing High β plasmas

S. M. Mahajan, Z. Yoshida, PRL **81**, 4863 (1998); Z. Yoshida, S. M. Mahajan, PRL **88**, 095001 (2002).

* Flow control is not conducted at present.

Starting from equations of motion of an electron and an ion

$$\mathbf{E}+\mathbf{v}_e\times\mathbf{B}+\frac{1}{m_e n}\nabla p_e=0 \quad \text{(inertia term neglected)}$$

$$\frac{\partial}{\partial t}\mathbf{v}_i+(\mathbf{v}_i\cdot\nabla)\mathbf{v}_i=\frac{e}{m_i}(\mathbf{E}+\mathbf{v}_i\times\mathbf{B})-\frac{1}{m_i n}\nabla p_i, \quad \text{we have}$$

$$\partial_t\mathbf{A}=(\mathbf{v}-\nabla\times\mathbf{B})\times\mathbf{B}-\nabla(-\phi+\varepsilon p_e) \quad \text{and}$$

$$\partial_t(\varepsilon\mathbf{v}+\mathbf{A})=\mathbf{v}\times(\mathbf{B}+\varepsilon\nabla\times\mathbf{v})-\nabla(\varepsilon v^2/2+\phi+\varepsilon p_i),$$

by using relations $\mathbf{E}=-\partial\mathbf{A}/\partial t-\nabla\phi$ and $\mathbf{j}=e(\mathbf{v}-\mathbf{v}_e)=1/\mu_0\nabla\times\mathbf{B}$

Taking curl, $\partial_t\mathbf{v}+(\mathbf{v}\cdot\nabla)\mathbf{v}=(\nabla\times\mathbf{B})\times\mathbf{B}-\nabla p$ and

$$\partial_t\mathbf{B}=\nabla\times[(\mathbf{v}-\varepsilon\nabla\times\mathbf{B})\times\mathbf{B}].$$

One of the time independent solutions is given by

$$\mathbf{B}=a(\mathbf{v}-\nabla\times\mathbf{B}) \quad \text{and} \quad \mathbf{B}+\nabla\times\mathbf{v}=b\mathbf{v}$$

This solution satisfies $v^2/2+p_i+\phi=const.$ and $p_i-\phi=const.$

Then the generalized Bernoulli condition $\beta+v^2=const.$ is derived.

Assuming that $\beta=0$ at the plasma surface and v is given by $\mathbf{E}\times\mathbf{B}$ speed, $E_r/B=v_A\beta^{1/2}$.

➡ Possibility of Ultra-high β (including $\beta>1$) equilibrium state of plasmas balanced by the dynamic pressure of plasma flow, when the plasma flow has a fast flow comparable to the Alfvén velocity v_A.

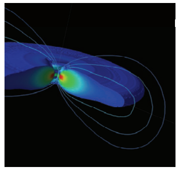

High β rotating plasma in Jupiter's magnetosphere

J. Shiraishi, Z. Yoshida et al., Pop 12, 092901 (2005).

II. Magnetospheric device Ring Trap 1 (RT-1)

The Ring Trap 1 (RT-1) device

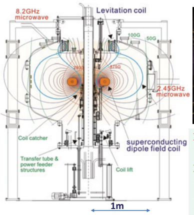

Cross section of RT-1: Magnetospheric configuration generated by a levitated superconducting magnet

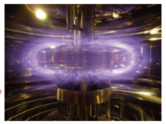

- Plasma formation by ECH
  - 2.45GHz (20kW) and 8.2GHz (25kW)
- Diagnostic system includes
  - 75GHz (4mm) interferometer
  - Visible light spectroscopy
  - Diamag loops and magnetic probes
  - SiLi and CdTe x-ray detectors
  - Soft x-ray CCD camera
  - Edge Langmuir probes

High-Tc superconducting coil

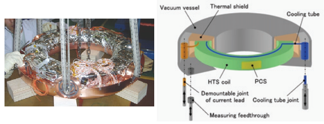

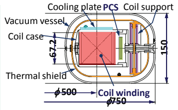

Main Parameters of the Floating HTS Coil

Winding method		Single pancake
Stack number of pancakes		12
Dimension	Major diameter	ϕ500 mm
	Hight	67.2 mm
Operating temperature		20~30 K
Magnetomotive force		250 kA
Operating current		115.6 A
Inductance		3.3 H
Stored energy		22 kJ

- Dipole field coil with Bi-2223 wires, PCS with YBCO (same as that of JR maglev).
- Cooled to 16K by GM refrigerators, 8 hours of operation.

III. High-β plasma formation

Yano *et al.*, to be submitted.

High β (hot electron) plasma

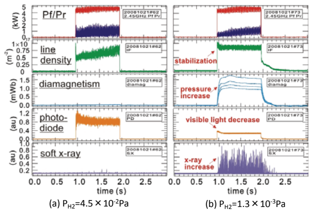

(a) $P_{H2}=4.5\times10^{-2}$Pa (b) $P_{H2}=1.3\times10^{-3}$Pa

Typical wave forms 2.45GHz ECH plasma (a) $P_{H2}=4.5\times10^{-2}$Pa (b) 1.3×10^{-3}Pa.

- Electrons consists of multiple temperatures.
- Plasma pressure mainly results from hot component (Te~10keV: SiLi detectors).

Energy confinement time

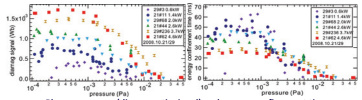

Plasma pressure (diamagnetic signal) and energy confinement time

- Hot electron population reaches ~30% by reducing neutral gas pressure.

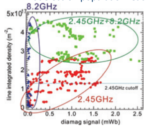

8.2/2.45GHz ECH

- Energy confinement time estimated from from stored energy and injected RF power is τ_{e1}~60ms.
- τ_{e1} approxmately agrees with magnetic measurement (diamag-decay time) of τ_{e2}~100ms.
- The stored energy is typically higher For 2.45GHz ECH

Effects of coil levitation

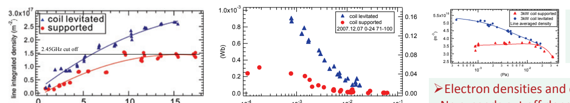

- Difference is clear when mean free path of an electron is longer than device scale.
- Electron densities and diamag signals
  - Ne exceeds cut off density, (suggests mode conversion to EBW).

Grad-Shafranov equilibrium analysis

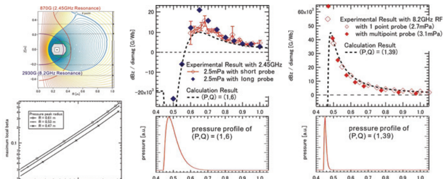

Hot electrons

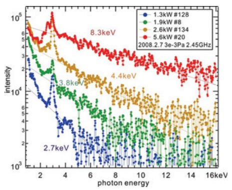

IV. Soft x-ray measurements with CCD camera

Plasma Fusion Res. **4**, 050 (2009).

X-ray CCD camera

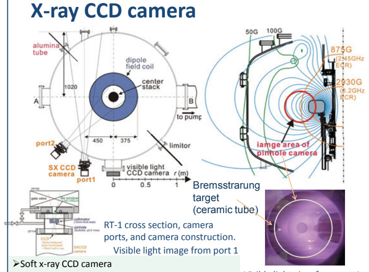

RT-1 cross section, camera ports, and camera construction.

Visible light image from port 1

Visible light view from port1

- Soft x-ray CCD camera
  - 1024×1024 pixel (13×13mm), 16bit dynamic range
  - Be window (100um), collimator, tantalum pinhole

Imaging mode of CCD camera

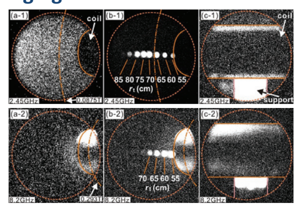

Soft x-ray images observed from (a) port 1, (b) port 1 with insertion of target tube At different radial positions, and (c) port2. (1) 2.45GHz and (b) 8.2GHz ECH.

- 2.45GHz: hot electrons fill approximately entire region in the image circle
  - 8.2GHz: x-ray emitting region localized near the coil, some lost on coil surface
- Coil support structure is the main loss channel of hot electrons for both cases

Photon counting mode

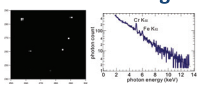

Enlarged CCD image and pulse height analysis

- Pulse height analysis of photon energies
- Impurity lines are used for energy calibration
- main loss channel of hot electrons for both cases
- T_e is approximately constant in the image circle

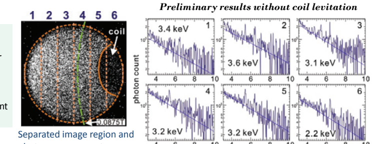

Separated image region and photon energy spectrum

Preliminary results without coil levitation

* Y. Liang *et. al.*, Rev. Sci. Instrum. **72**, 717 (2001); PFR **4**, 050 (2009).

V. Stable confinement of toroidal non-neutral plasma

Electron beam injection

Yoshida *et al.*, submitted to PRL.

- Test of particle transport properties using NNP
  - Inward particle diffusion is theoretically predicted in dipole devices.
  - Physics of flowing plasmas single-component.
- Trapping of non-neutral plasma in toroidal geometry
  - Requires no axial potential well, in contrast to linear traps.
  - Capable of trapping plasmas with arbitrary non-neutrality.
  - Potential applications for antimatter plasmas (currently only electrons).

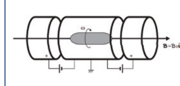

Linear configuration for non-neutral Plasmas (Penning-mlmberg trap, etc.)

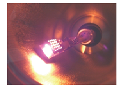

Stabilization and long confinement

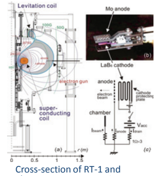

Cross-section of RT-1 and Electron gun construction

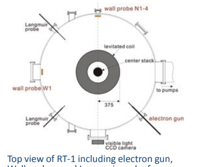

Top view of RT-1 including electron gun, Wall probes, and Langmuir probe for pure electron plasma experiment

- Electrons are injected from an electron gun located at the edge region.
- Electrons are initially accelerated between cathode ($-V_{acc}$) and anode (0V).

Visualized magnetic surfaces

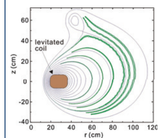

Single-particle orbits of electron Projected on r-z cross section of RT-1

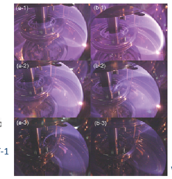

$$P_\theta=\frac{\partial L}{\partial\dot\theta}=mr^2\dot\theta+qrA_\theta=const.$$

$$L=\frac{mv^2}{2}+q\mathbf{v}\cdot\mathbf{A}-q\phi$$

$$d\le\left|mr\dot\theta/qB_p\right|$$

- In pure poloidal field of RT-1, single particle orbits are localized near the initial magnetic surfaces (r_L<6mm).
- Visualized surfaces agrees with calculated vacuum magnetic surfaces

Long confinement

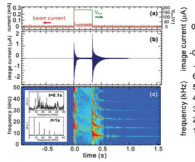

Waveforms during and just after beam injection

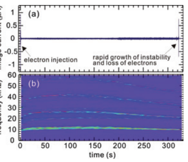

Fluctuation during long confinement

- The fluctuation spectrum has large-amplitude, broad, and multiple peaks during electron injection.
- With coil levitation, the fluctuation stabilizes and the plasma is trapped for more than 300s.
- Coherent fluctuation suggests rigid rotation, in spite of strongly inhomogeneous field strength.

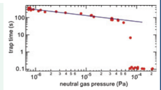

Stable confinement time

VI. Observation of inward particle diffusion (NNP)

Estimated confinement region

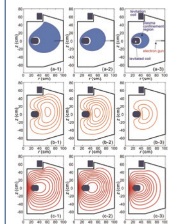

(a) Confinement regions, (b) potential profiles measured by wall probes, and (c) total potential Profiles (1) during electron injection (2) just after injection ends (3) just Before confinement ends.

- Confinement region gradually shifts inward:
  - During beam injection, approximately whole region inside the separatrix are filled.
  - Plasma on magnetic surfaces intersecting the gun structure is rapidly lost.
  - Plasma stably trapped in strong field region.
- Electrons deviates from initial magnetic surfaces, transported to strong field region.

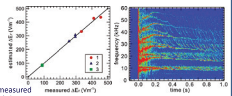

Values of electric field strength measured by Wall probes and generated by electron clouds.

Perturbation-free E_r measurement by wall probe

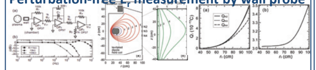

$$V_{o2}=-\frac{R_1R_3}{C_1R_2R_3}\int I_d dt=-1.06\times10^{10}Q_i$$

$$E_r=-\int I_d dt/\varepsilon_0 S=5.33\times10^3\times V_{o2}$$

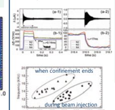

- Reconstruction methods of plasma profiles
- We used following assumptions:
  - Plasma is toroidally symmetric and, has constant density.
  - Magnetic surfaces give boundaries (dotted line inside).
  - Coil voltage (V_c) is constant.
- By changing external boundary surface, image density profiles are modified, which is detected by wall probes.
- For various external boundary positions ($r=r_0$), values of $(Q_{N2}/Q_{N4})^2+(Q_{N3}/Q_{N4})^2$ are calculated.
- Plasma external boundary (r_0) can be uniquely decided.

Plasma Fusion Res. **4**, 050 (2009).

Space potential exceeds V_{acc}

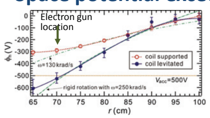

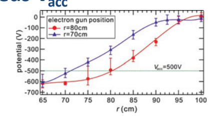

- Space potential at $r<r_{gun}$ (in the stronger field region) is lower than V_{acc}, indicating inward transport and energization of electrons.
- Flow (toroidal E × B drift) has strong shear, especially when the coil is supported and the plasma has turbulence-like fluctuations.

Fluctuation-induced radial transport

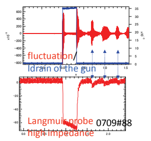

(a) Cathode voltage and fluctuation.
(b) Langmuir probe measurement.

- Radial transport and onset of instability was simultaneously observed.
- Langmuir probe was used as particle flux probe located at r=85cm.
- Electrons were injected from gun located at r=80cm.

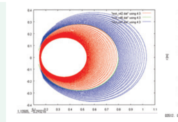

Resonance particle orbits including azimuthal electric field ~10^4V/m

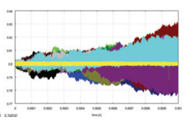

Radial transport of electrons due to random electric field.